NJC

Accepted Manuscript

This is an *Accepted Manuscript*, which has been through the Royal Society of Chemistry peer review process and has been accepted for publication.

Accepted Manuscripts are published online shortly after acceptance, before technical editing, formatting and proof reading. Using this free service, authors can make their results available to the community, in citable form, before we publish the edited article. We will replace this *Accepted Manuscript* with the edited and formatted *Advance Article* as soon as it is available.

You can find more information about *Accepted Manuscripts* in the Information for Authors.

Please note that technical editing may introduce minor changes to the text and/or graphics, which may alter content. The journal's standard Terms & Conditions and the Ethical guidelines still apply. In no event shall the Royal Society of Chemistry be held responsible for any errors or omissions in this *Accepted Manuscript* or any consequences arising from the use of any information it contains.

ROYAL SOCIETY OF CHEMISTRY

www.rsc.org/njc

Journal Name

RSCPublishing

ARTICLE

Effect of hydrogen bond on supramolecular self-aggregation mode and extent of metal-free benzoxazole-substituted phthalocyanines

Cite this: DOI: 10.1039/xoxxoooooox

Received ooth January 2012,
Accepted ooth January 2012

DOI: 10.1039/xoxxoooooox

www.rsc.org/

Yinghui Bian, Jinshe Chen, Shaotang Xu, Yulu Zhou, Lijun Zhu, Yuzhi Xiang and Daohong Xia*

Two novel metal-free phthalocyanines have been designed and synthesized, namely tetra{[1H-benzo(*d*)imidazol-2-yl]thiol}phthalocyanine (TBIT-Pc) and tetra{[benzo(*d*)thiazol-2-yl]thiol}phthalocyanine (TBTT-Pc). These two compounds showed similar structures, while imidazolyl-NH in the substitutes of TBIT-Pc could form more hydrogen bonds. TBIT-Pc and TBTT-Pc were fully characterized by elemental analysis, ^{1}H NMR, MALDI-TOF MS, FT-IR and UV-Vis absorption spectrum. The self-assembly properties of TBIT-Pc and TBTT-Pc were comparatively studied. TBIT-Pc and TBTT-Pc were present as monomer in DMF in the concentration range of 9.04~20.3 μM. Depending mainly on the intermolecular hydrogen bonding (N-H···N) between benzimidazole substitutes, "head-to-tail" J-aggregates of TBIT-Pc were formed in DMSO, while there is no aggregation of TBTT-Pc in the same solvent. "Face-to-face" H-aggregates of TBIT-Pc and TBTT-Pc were formed with the addition of water to the solutions of DMSO, and the degree of aggregation increased with the introduction of H-bonds (N-H···N) in the benzimidazole substitutes of TBIT-Pc. The Atomic Force Microscope (AFM) image and Dynamic light scattering (DLS) displayed the formation of well-defined nanoparticles with a diameter of ca. 30±15 nm with J-type aggregation of TBIT-Pc. And the dendritic nanostructures with H-aggregates of TBIT-Pc and TBTT-Pc with different size were observed from Transmission Electron Microscopy (TEM) images. The possible mechanism of the effect of H-bonds on the formation of J-aggregates of TBIT-Pc and the H-aggregation of TBIT-Pc and TBTT-Pc was also discussed. In the formation process of aggregates, H-bonds and π-π interaction may be the dominant factors. In addition, the nanostructures fabricated from TBIT-Pc and TBTT-Pc showed good semiconducting properties revealed by current-voltage measurements.

Introduction

Phthalocyanines (Pcs) are remarkable compounds possessing photophysical,[1] semiconducting,[2] and photoconducting properties due to their 18π-electron aromatic macrocyclic structure.[3,4] Phthalocyanines have been used as dyes and pigments first of all.[5-7] Because of their excellent thermal stability and visible area optical properties, phthalocyanines are also ideal for applications in sensors,[9,10] electronic displays,[4] non-linear optical devices,[11] solar cells,[12] semi-conductors,[13] data storage systems,[14] catalysts[15] and as photodynamic therapy (PDT) agents.[16] One of the most important properties of phthalocyanines is self-assembly or aggregation in solutions. The aggregation of phthalocyanines is similar to porphyrins which exist in petroleum and affect the aggregation properties of petroleum fractions. And the aggregation is interesting and significant in many chemical[17] and biochemical[18] systems, since strong association interaction between molecules. The phthalocyanine structure incorporation with various substituents has been shown not only to enhance their solubility, but also affect their self-assembly effectively.

The self-assembly or aggregation of phthalocyanines can be achieved through the cooperation of intermolecular interactions such as π-π stacking, hydrogen-bond, acid-base interactions, and donor-acceptor interactions.[19-22] As well known, "head-to-tail" J-type stacking and "face-to-face" H-type stacking of aggregates are observed in phthalocyanines.[23,24] Species with the absorption bands shifted to the blue relative to the monomer absorption are termed H-aggregates, while species with absorption bands red-shifted are termed J-aggregates.[25,26] H-aggregates as the predominant component of self-assembly of phthalocyanines are known to be non-photoactive, while J-type aggregates with photoactivity are rarely observed.[27,28] To reliably change the stacking process or mode of phthalocyanines self-assembly, the hydrogen bond is an ideal candidate due to its directionality and reversibility.[29] Shinkai

and coworkers[30] have found that the hydrogen bonding interactions among saccharide groups are able to finely change the face-to-face orientation mode of porphyrin molecules, resulting in the formation of H- or J-aggregates in an organogel system. Among the substituted phthalocyanines, the heterocyclic group has been received considerable attention.[31] In addition, imidazole and thiazole derivatives contain nitrogen and sulphur atoms which could form hydrogen-bonding among different phthalocyanine molecules. Recently, imidazole substituted porphyrins and phthalocyanines have been synthesized[32-37] and investigated for their optical property,[33] electrical property,[34] electron transfer processes[35], catalytic property[36] and molecular switch properties.[37] However, few researches on the comparative study of self-assembly properties of imidazole and thiazole substituted phthalocyanines have been reported. The -NH in imidazole substituted phthalocyanines could increase the number of N-H···N hydrogen bonds between neighboring Pcs molecules. And the self-assembly mode will be varied compared to thiazole-substituted phthalocyanines.

In this work, we described the design and synthesis of two new phthalocyanine derivatives, namely tetra{[1H-benzo(*d*)imidazol-2-yl]thiol}phthalocyanine (TBIT-Pc, 6) and tetra{[benzo(*d*)thiazol-2-yl]thiol}phthalocyanine (TBTT-Pc, 7), as shown in Scheme 1. The self-assembly properties of TBIT-Pc and TBTT-Pc at different concentrations and in different solvents were comparatively investigated. The results indicated the great effect of hydrogen bonds on the self-assembly mode and aggregation degree. The semiconducting property of these nano-aggregates was also explored.

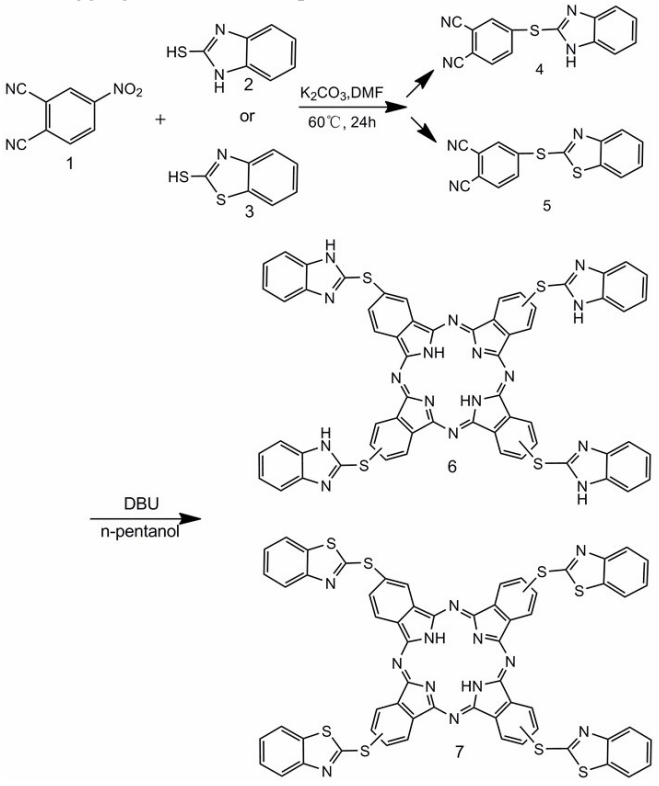

Scheme 1. Synthetic route of novel tetra{[1H-benzo(*d*)imidazol-2-yl]thiol}phthalocyanine (TBIT-Pc, 6) and tetra{[benzo(*d*)thiazol-2-yl]thiol}phthalocyanine (TBTT-Pc, 7) .

Experimental

Materials

2-Mercaptobenzimidazole (2), 2-mercaptobenzothiazole (3) and 1,8-diazabicyclo[5.4.0]undec-7-ene (DBU) were purchased from Aladdin. DMF and n-pentanol were freshly distilled just before use. The progress of the reactions was monitored by TLC (SiO_2). Column chromatography was carried out on silica gel (Haiyang, Kieselgel 60, 200-300 mesh) with the selected eluents. 4-Nitrophthalonitrile (1) was synthesized according to the reported literature[38].

Instruments

The ^{1}H NMR (600 MHz) spectra were recorded on a Bruker AVANCE III 600 in $CDCl_3$ and DMSO-d_6 solutions. MALDI-TOF mass spectrum was taken on a Bruker BIFLEX III and Elemental analysis was performed on an Elementar Vario EL III instrument. The FT-IR spectra were recorded with a Nicolet 6700 Fourier transform infrared instrument. The UV-Vis spectra were measured on a Hitachi U-3900H spectrophotometer. Fluorescence emission spectra were recorded on a Horiban Jobin Yvon FluoroMax-4 spectrofluorometer. AFM images of the aggregates were performed with a commercial Nanoscope IVa MultiMode atomic force microscope. TEM images of the aggregates were performed on a JEOL 1200EX electron microscopy. The size measurements of nanoaggregates were carried out by Dynamics light scattering (DLS) technique.

Syntheses

Phthalonitrile derivatives (4-5). 2-Mercaptobenzimidazole (2) (1.50 g, 0.01 mol) or 2-mercaptobenzothiazole (3) (1.67 g, 0.01 mol) were added to the DMF solution (25 mL) of 4-nitrophthalonitrile (1) (1.73 g, 0.01 mol), respectively. Then the mixture solution was stirred at 55-60 ℃ under N_2 stream. Powdered anhydrous potassium carbonate (K_2CO_3) (1.38 g, 0.01 mol) was added in eight equal portions over 2 h and the mixture was stirred vigorously at the same temperature for further 24 h. After one day, the reaction mixture was poured into ice-water (200 mL). The precipitate formed was filtered and washed successively with water until the washing became neutral and then washed with methanol three times. Finally, the crude product was crystallized repeatedly from ethanol.

4-{[1H-benzo(*d*)imidazol-2-yl]thio}phthalonitrile (4). Grayish crystalline powder. Yield: 65% (1.8 g), MA=276.2 g/mol, m.p.=158℃. ^{1}H NMR (600 MHz, DMSO-d_6) (δ: ppm): δ 13.22 (s, 1H, -NH), 8.28 (d, J = 1.8 Hz, 1H, Ar-H), 8.10 (d, J = 8.4 Hz, 1H, Ar-H), 7.83 (dd, J = 8.4, 1.9 Hz, 1H, Ar-H), 7.61 (s, 2H, Ar-H), 7.28 (dd, J = 5.7, 2.8 Hz, 2H, Ar-H). MS (ESI), (m/z): 277.1 $[M+H]^+$. For $C_{15}H_8N_4S$ Anal. Calc.: C, 65.15; H, 2.90; N, 20.27. Found: C, 67.52; H, 2.83; N, 21.04%.

4-[benzo(*d*)thiazol-2-ylthio]phthalonitrile (5). Oyster crystalline powder. Yield: 65% (1.92 g), MA=293.2 g/mol, m.p.=159℃. ^{1}H NMR (600 MHz, $CDCl_3$) (δ: ppm):δ 8.06-7.98 (m, 2H, Ar-H), 7.92 (dd, J = 8.2, 1.7 Hz, 1H, Ar-H), 7.85 (d, J = 8.0 Hz, 1H, Ar-H), 7.79 (d, J = 8.3 Hz, 1H, Ar-H), 7.53 (t, J = 7.7 Hz, 1H, Ar-H), 7.45 (t, J = 7.6 Hz, 1H, Ar-H). MS (ESI), (m/z): 294.0 $[M]^+$. For $C_{15}H_7N_3S_2$ Anal. Calc.: C, 61.35; H, 2.39; N, 14.31. Found: C, 59.68; H, 2.45; N, 13.89%.

Metal-free phthalocyanines (6-7). 4-{[1H-benzo(*d*)imidazol-2-yl]thio}phthalonitrile (4) (0.218 g, 0.79 mmol) or 4-[benzo(*d*)thiazol-2-ylthio]phthalonitrile (5) (0.232 g, 0.79 mmol) were dissolved in 5 mL n-pentanol, respectively. The mixed solution was heated at 90℃ under N_2 and DBU (0.44 mL, 0.8 mmol) was added to the mixed solution. Then the reaction mixture was heated to 138℃ and stirred at this temperature for 24 h under N_2. The dark blue mixture was diluted with 30 mL n-hexane and stirred for 12 h after cooling to room temperature. The precipitated was filtered off and washed with methanol, ethanol, aether, successively. Finally, pure metal-free phthalocyanines were obtained by column chromatography on silica gel using CH_3COCH_3/THF (10/1, v/v), CH_3COCH_3/CH_2Cl_2 (10/1, v/v) as eluent for compound 6 and compound 7, respectively.

Tetra{[1H-benzo(*d*)imidazol-2-yl]thiol}phthalocyanine (6). Yield: 32% (0.28 g), m.p. >300 ℃. IR ν_{max}/(cm^{-1}): 3296, 3051, 1609, 1483, 1469, 1449, 1236, 1162, 1104, 1011, 927, 877, 851, 761. UV/Vis (DMF): λ_{max} nm (log ε) 719 (4.51), 677 (4.49). ^{1}H NMR (600 MHz, DMSO-d_6) (δ: ppm): 12.42 (s, 4H, Im-NH), 8.78-7.38 (m, 28H, Ar-H). MALDI-TOF MS: Calculated: 1107.3 [M]; Found: 1106.9 $[M]^+$. For $C_{60}H_{34}N_{16}S_4$ Anal. Calc.: C, 65.07; H, 3.07; N, 20.20. Found: C, 64.88; H, 3.08; N, 20.27%.

Tetra{[benzo(*d*)thiazol-2-yl]thiol}phthalocyanine (7). Yield: 33% (0.31 g), m.p. >300 ℃. IR ν_{max}/(cm^{-1}): 3288, 3052, 1602, 1491, 1463, 1441, 1238, 1159, 1101, 1019, 926, 870, 850, 758. UV/Vis (DMF): λ_{max} nm (log ε) 714 (4.57), 675 (4.59). ^{1}H NMR (600 MHz, DMSO-d_6) (δ: ppm): 8.56-7.58 (m, 28H, Ar-H). MALDI-TOF MS: Calculated: 1175.4 [M]; Found: 1174.7 $[M]^+$. For $C_{60}H_{30}N_{12}S_8$ Anal. Calc.: C, 61.30; H, 2.55; N, 14.30. Found: C, 61.58; H, 2.54; N, 14.26%.

Results and discussion

Design, synthesis and characterization of TBIT-Pc and TBTT-Pc

Imidazole and thiazole derivatives substituted phthalocyanines have been received considerable attention. The -NH in benzimidazole substitutes of phthalocyanines could increase the number of N-H···N hydrogen bonds between neighboring Pcs molecules. The self-assembly stacking mode and aggregation degree will be different from thiazole substituted phthalocyanines. Therefore, mercaptobenzimidazole and mercaptobenzothiazole have been chosen as the peripheral substituents of phthalocyanines in this paper. The synthesis route of tetra{[1H-benzo(*d*)imidazol-2-yl]thiol} phthalocyanine (TBIT-Pc, 6) and tetra{[benzo(*d*)thiazol-2-yl]thiol} phthalocyanine (TBTT-Pc,7) was shown in scheme 1. In the synthetic procedure, the first step was to obtain 4-{[1H-benzo(*d*)imidazol-2-yl]thio} phthalonitrile (4) and 4-[benzo(*d*)thiazol-2-ylthio] phthalonitrile (5) as precursors of phthalocyanines. Then metal-free phthalocyanines (TBIT-Pc and TBTT-Pc) were obtained respectively by cyclotetramerization of compound 4 and compound 5 in dry n-pentanol in the presence of DBU under N_2 atmosphere with reflux for 24 h. The phthalocyanines were purified through column chromatography. The MALDI-TOF mass spectra of the obtained compounds clearly showed intense signal corresponding to the molecular ion M^+. The compounds were further characterized by ^{1}H NMR, FT-IR and UV-Vis spectroscopic methods. Due to the presence of four polar peripheral substituents,[39] both TBIT-Pc and TBTT-Pc exhibited excellent solubility in DMF, THF and DMSO. TBTT-Pc also showed good solubility in chloroform. However, their solubility in some organic solvents, such as methanol, ethanol, acetone, dichloromethane and toluene is limited.

Electronic absorption of TBIT-Pc and TBTT-Pc

As well known, phthalocyanines exhibit characteristic absorption spectra with two distinguished wavelength ranges. One is termed ''B'' or Soret band (approx. 300–400 nm) and the other one is called as the ''Q'' band (approx. 600-800 nm).[7,40] Due to D_{2h} symmetry, the Q bands of metal-free phthalocyanines are splitted into Q_x and Q_y bands.[41] The absorption spectra of TBIT-Pc and TBTT-Pc in DMF at the concentration of 2.03×10^{-5} M are shown in Fig.1. Similar absorption spectra were observed for TBIT-Pc and TBTT-Pc. The B-bands for TBIT-Pc and TBTT-Pc in the UV region were at about 350-370 nm. And the metal-free TBIT-Pc and TBTT-Pc gave a split Q-band of high intensity at about 715 (Q_x) and 670 nm (Q_y), indicating the obtained structure with non-degenerate D_{2h} symmetry.[42-44] The characteristic absorption spectra for the synthesized phthalocyanines were also observed in the DMSO and THF solutions of TBIT-Pc and TBTT-Pc (Fig. S1).

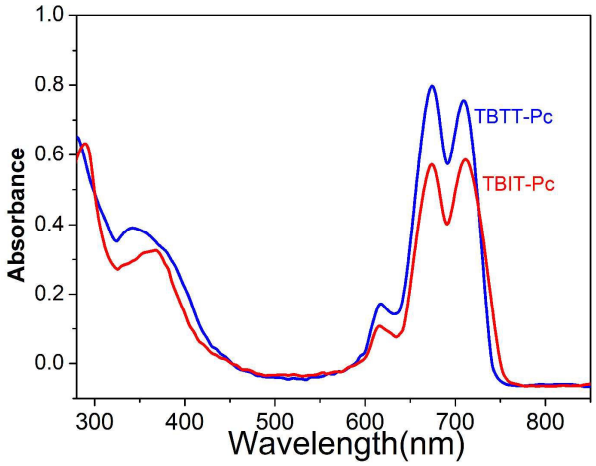

Fig.1. Electronic absorption spectra of TBIT-Pc (red) and TBTT-Pc (blue) in DMF at 2.03×10^{-5} M.

Phthalocyanines have generally high tendency of aggregation due to their specific 18 π-electron systems. The self-aggregation has a significant effect on their optical and electrochemical properties.[45,46] For phthalocyanines, the self-assembly behavior in solution is a good indication of the presence of interactions between different molecules.[47] Aggregation is usually investigated by the electronic absorption spectrum depending on the concentration varied.[48-50] For the aggregation of phthalocyanine, the Q band exhibits a blue-shift or red-shift with some decrease in intensity.[51] The aggregation behavior of the metal-free TBIT-Pc and TBTT-Pc were investigated at different concentrations in DMF. As shown in Fig.2, in the concentration range of 9.04×10^{-6}~20.3×10^{-6} M, intensity of the Q-band gradually increased with an increase of concentration. Meanwhile, there were no new bands (normally blue shifted) due to the aggregated species for TBIT-Pc (Fig.2a) and TBTT-Pc (Fig.2b). It indicated that TBIT-Pc and TBTT-Pc were mostly present as monomer in DMF and obeyed the Beer-Lambert law in the tested concentration range.[52]

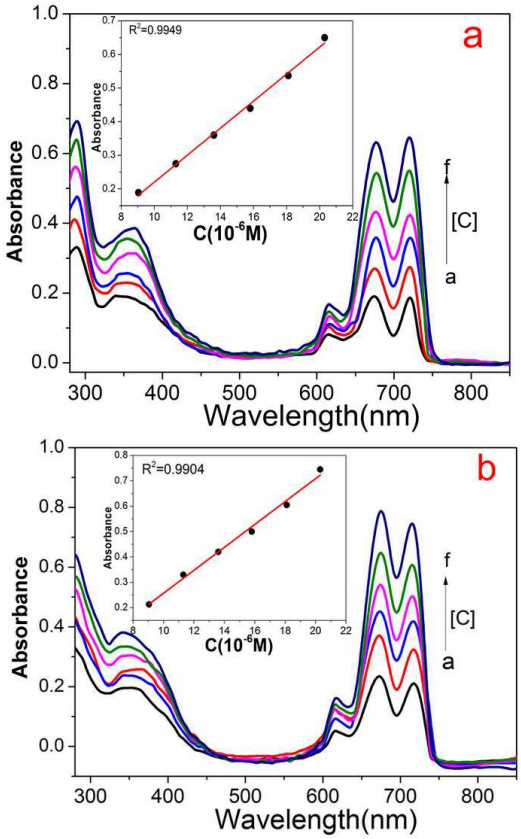

Fig.2. Electronic absorption spectra for TBIT-Pc (A) and TBTT-Pc (B) in DMF at different concentrations (a-f): 9.04×10^{-6}, 11.3×10^{-6}, 13.6×10^{-6}, 15.8×10^{-6}, 18.1×10^{-6}, 20.3×10^{-6} M. (Insets: Plot of absorbance versus concentration in Q-band.)

The formation of phthalocyanine aggregates is also solvent-dependent.[53] Kimura and coworkers[54] have studied the self-organizing properties of novel amphiphilic metallophthalocyanines in DMSO-water mixtures with different water content. The aggregated phthalocyanine species with a cofacial arrangement formed in the solutions. Thus, the aggregation behavior of TBIT-Pc and TBTT-Pc was studied in DMSO and mixtures of water and DMSO (1/1, v/v) as a result of solvent effect. The concentration of TBIT-Pc and TBTT-Pc was kept constant at 1.58×10^{-5} M. As can be seen from Fig.3a, the Q-band absorption spectrum of TBIT-Pc in DMSO was significantly different from that in DMF. In comparison with the monomer in DMF, the Q-band of TBIT-Pc in DMSO after stabilization showed a remarkable red shift, which is the typical characteristic of the formation of J-aggregation.[26] However, TBTT-Pc was also present as monomer in DMSO because the spectrum was similar to those of its monomer in DMF. The color of the DMSO solution of TBIT-Pc was different from TBTT-Pc as shown in the insets of Fig.3. This was quite reasonable because of the different forms in existence. These results indicate that the presence of hydrogen bonding (N-H···N) between benzimidazole substitutes of TBIT-Pc affect the formation of aggregation in DMSO solutions effectively. The electronic absorption spectra of TBIT-Pc and TBTT-Pc in DMSO/water are also given in Fig. 3. With respect to the monomer, the absorption of TBIT-Pc and TBTT-Pc in DMSO/water at 710 nm decreased and a new blue-shifted band appeared, both of which indicated the formation of H-aggregates promoted by the addition of water.[55] In detail, the Q band took a remarkable blue shift of 60 nm for TBIT-Pc in DMSO/water. However, a slight blue shift of 10 nm was observed for TBTT-Pc in DMSO/water, indicating that the extent of H-aggregation increased with the introduction of hydrogen bonds (N-H···N) between benzimidazole substitutes of TBIT-Pc. The images of the H-aggregates formed also showed aggregates in existence with larger size in DMSO/water mixture of TBIT-Pc than TBTT-Pc, which agreed with the results of Q-band absorption spectra.

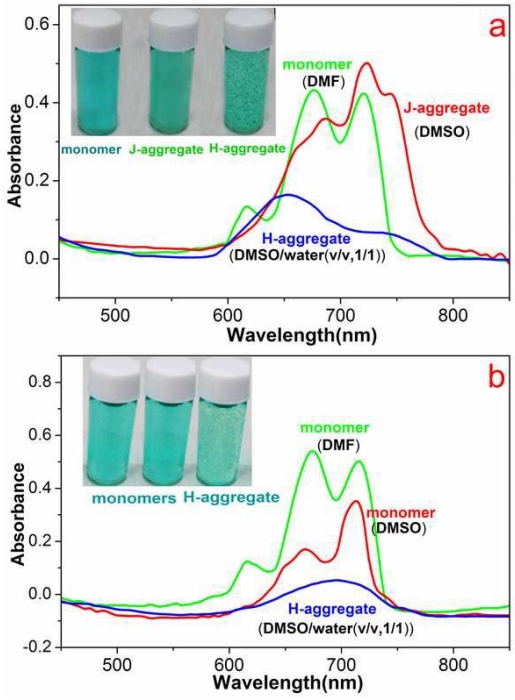

Fig.3. Q-band absorption spectra of TBIT-Pc (a) in the form of monomer (in DMF), J-aggregate (in DMSO, 6 h after dissolving solid sample), H-aggregate (DMSO/water mixture, 1/1, v/v) and TBTT-Pc (b) in the form of monomer (in DMF and DMSO), H-aggregate (DMSO/water mixture, 1/1, v/v). Insets: Images of (a) monomer, J-aggregate, H-aggregate and (b) monomers, H-aggregate. The concentration of TBIT-Pc and TBTT-Pc was kept constant at 1.58×10^{-5} M.

J-aggregation of TBIT-Pc in DMSO

The electronic absorption spectra and fluorescence spectra of TBIT-Pc in DMSO are given in Fig.4. As shown in the electronic absorption spectra of TBIT-Pc in DMSO (Fig.4a), the spectrum displayed a broad and single Q band at 715 nm at the concentration of 9.04×10^{-6} M. The absorption at 715 nm gradually increased with increasing concentration and the new red-shifted band gradually appeared at 741 nm. According to the Kasha's exciton theory,[56] the new bands observed for TBIT-Pc in DMSO are attributed to the head-to-tail aggregates, or so-called J-aggregates. The corresponding fluorescence spectra obtained at an excitation wavelength of 640 nm are displayed in

Fig. 4b. The high intensity at 721 nm increased with the concentration increasing from 9.04×10^{-6} M to 11.3×10^{-6} M, while decreased slightly in the concentration range of 11.3×10^{-6} ~20.3×10^{-6} M. A new red-shifted emission band gradually appeared at 741 nm. The significant red-shift of emission bands were observed for the DMSO solution of TBIT-Pc, which also indicated the formation of J-aggregates promoted by hydrogen bonds between different phthalocyanine molecules. The quantum yield of the emission was evaluated to be 0.55 using that for metal-free phthalocyanine (0.85) as the standard.[57] This result supported that J-aggregates of TBIT-Pc were fluorescent.

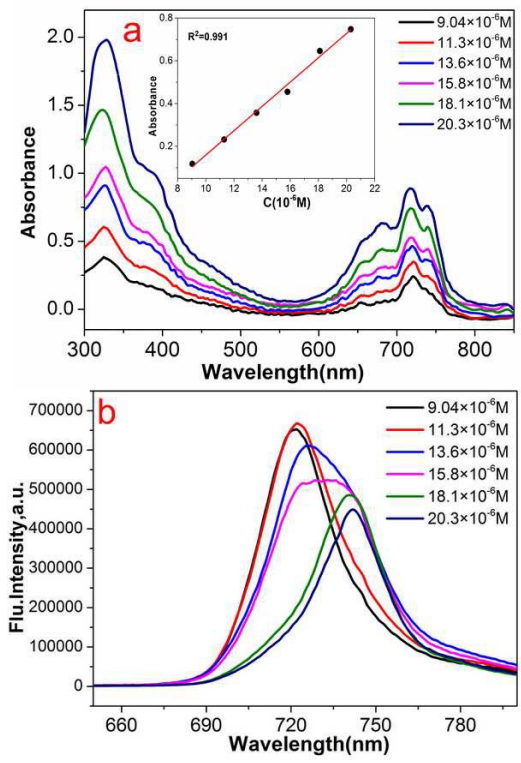

Fig.4. Electronic absorption spectra (a) and fluorescence spectra (b) of TBIT-Pc in DMSO at different concentrations. The inset of electronic absorption spectra shows the absorbance changes of Q-bands at 741 nm.

H-aggregation of TBIT-Pc and TBTT-Pc in DMSO/water mixture

The electronic absorption spectra and corresponding fluorescence spectra of TBIT-Pc and TBTT-Pc were studied in DMSO/water mixed solutions in various volume ratios (10:0～35:65(v/v)). The concentration of TBIT-Pc and TBTT-Pc was kept at 1.58×10^{-5} M. As shown in Fig. 5a, absorbance at the Q-band of TBIT-Pc decreased with increasing water content. And a new band with a great blue-shift of 50 nm (around 652 nm) appeared when water content was more than 30 vol%. These spectral changes may be attributed to the formation of H-type (face-to-face conformation) aggregations, which was promoted by the addition of water. The formation of H-aggregates has also been supported by fluorescence spectra, which were obtained at an excitation wavelength of 640 nm in Fig. 5b. The intensity at 726 nm decreased with increasing water content in the DMSO/water mixtures and a new blue-shifted band around 712 nm gradually appeared when water content was more than 20 vol%. The intensity at 712 nm further decreased down to baseline with the increasing water content, which indicated the new species formed with non fluorescence (observed from Fig. 5a). This is expected for the H-aggregates.[26] Fluorescence quantum yields (Φ_f) were also determined by metal-free phthalocyanine (Φ_f=0.85) as a standard.[57] Φ_f values for TBIT-Pc decreased dramatically from 0.55 in DMSO to 0.001 in DMSO/water. These results demonstrated that the stacking mode of TBIT-Pc in DMSO solution (J-aggregates) could be changed by adding water to the DMSO solutions.

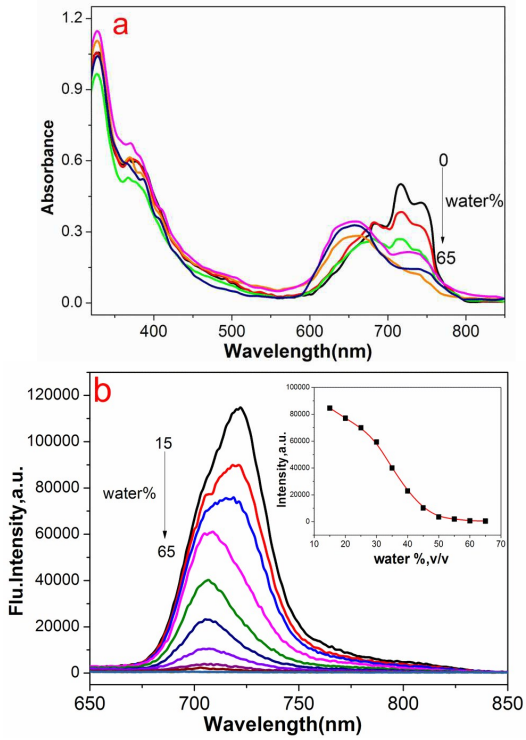

Fig.5. Electronic absorption spectra (a) and fluorescence spectra (b) of TBIT-Pc in DMSO/water mixed solution with different volume ratios. The concentration of TBIT-Pc was kept constant at 1.58×10^{-5} M. Inset: Dependence of fluorescence intensity on the content of water in the mixed solutions.

Similar changes of absorption and fluorescence spectra have been observed in DMSO/water mixed solutions for TBTT-Pc (Fig. 6). Upon aggregation of TBTT-Pc induced by the addition of water, the high intensity at 710 nm in monomer of TBTT-Pc also decreased and a new blue-shifted absorption band at 702 nm was observed. The difference in absorption spectra was that the aggregation bands of TBTT-Pc were recorded at higher wavelengths than that of TBIT-Pc. Meanwhile, the fluorescence intensity at 726 nm decreased down to baseline without the appearance of a new emission band, indicating the formation of non-fluorescent H-aggregates. Φ_f values for TBIT-Pc decreased dramatically from 0.60 in DMSO to 0.002 in DMSO/water. Thus, both TBIT-Pc and TBTT-Pc were strongly aggregated in DMSO/water mixed solutions and the degree of aggregation increased in the DMSO/water mixture of TBIT-Pc. These results indicated that H-bonds and strong interactions between π-clouds gave rise to H-aggregates of TBIT-Pc and TBTT-Pc.

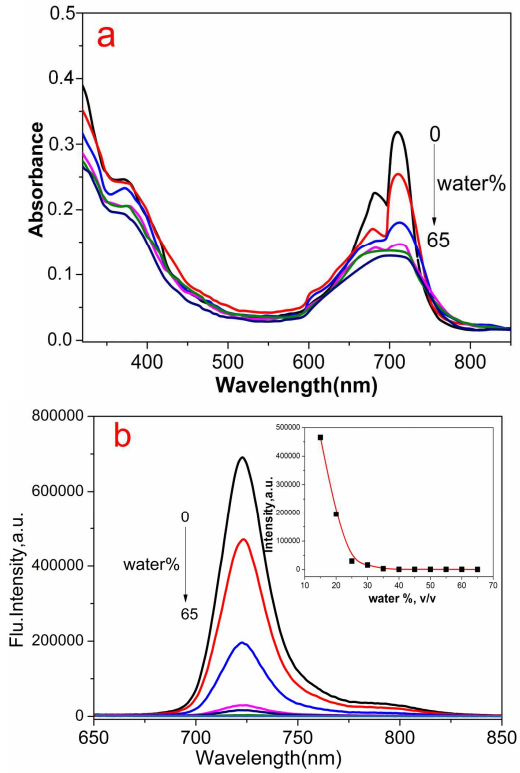

Fig.6. Electronic absorption spectra (a) and fluorescence spectra (b) of TBTT-Pc in DMSO/water mixed solution with different volume ratios. The concentration of TBTT-Pc was kept constant at 1.58×10^{-5} M.

Morphology of aggregates

Electronic absorption spectra and fluorescence spectra of TBIT-Pc and TBTT-Pc in DMSO and DMSO/water mixture described above revealed the formation of J- and H-aggregates. To characterize the dimensions and morphologies of the nanoaggregates, AFM have been recorded for J-aggregates fabricated from TBIT-Pc (Fig. 7a). TEM images have been recorded for H-aggregate of TBIT-Pc and TBTT-Pc formed in DMSO/water mixture (Fig. 7b and Fig. 7c). As shown in the AFM image (Fig. 7a), the TBIT-Pc molecules assembled into well-defined nanoparticles with a diameter of ca. 30±15nm. As displayed in the TEM image (Fig. 7c), TBIT-Pc molecules in DMSO/water mixture self-assembled into dendritic nanostructures with a length from 1000 to 150 nm and a width from 30 to 20 nm. In comparison with the nanostructure of TBIT-Pc H-aggregates, shorter dendritic nanostructures was formed in DMSO/water mixture of TBTT-Pc for which the length was from 600 to 200 nm and the width was from 20 to 10 nm (Fig.7d). Therefore, the results of AFM and TEM agreed with those by electronic absorption and emission spectra measurements. All the results establish the fact that J-aggregation and the increase of H-aggregation degree were induced by the hydrogen bonds (N-H···N) between benzimidazole substitutes of TBIT-Pc.

Dynamic light scattering (DLS) was also studied for estimation of the particle sizes of the TBIT-Pc J-aggregates formed in DMSO (Fig.7b). The spectra were analyzed for particle size distribution using the CONTIN algorithm.[58] It was found that the hydrodynamic diameter of nanoparticles formed in the DMSO solution of TBIT-Pc is mainly distributed in the range of 8~89 nm with an average hydrodynamic diameter of 30 nm, which is in good accordance with AFM measurements.

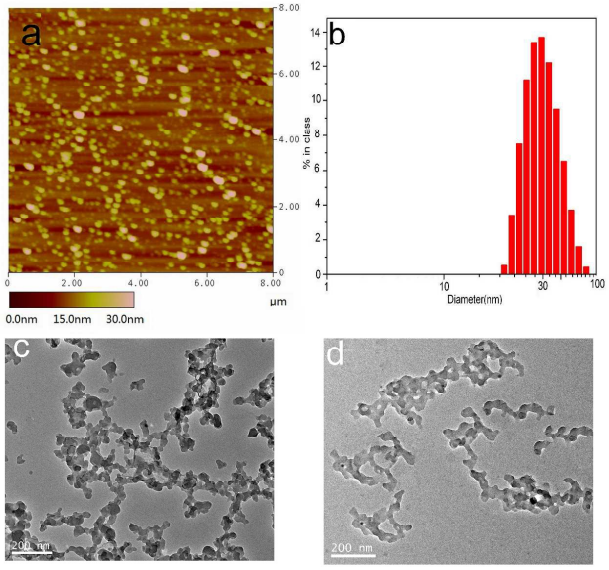

Fig.7. AFM (a) and TEM (c and d) images of the TBIT-Pc nanoaggregates in DMSO (a), DMSO/water (c) and TBTT-Pc nanoaggregates in DMSO/water (d) after 6h of aggregation. DLS results for TBIT-Pc in DMSO (b).

Mechanism of Self-Assemblies

On the basis of the electron absorption and fluorescence spectra, the possible mechanism of the TBIT-Pc J-aggregates formed in DMSO and H-aggregates formed in the DMSO/water mixture of TBIT-Pc and TBTT-Pc are described in Fig. 8. As shown in the electron absorption spectrum in Fig. 3b, TBTT-Pc was mainly present as monomer in DMSO, which was possibly due to the formation of intermolecular hydrogen bonds between TBTT-Pc molecules and DMSO molecules. However, the head-to-tail J-aggregates formed in DMSO solution of TBIT-Pc may be induced by the hydrogen bonds (N-H···N) between benzimidazole substitutes. After adding water to the DMSO solutions of TBIT-Pc and TBTT-Pc, water molecules would be linked with DMSO molecules via hydrogen bonds, which resulted in the disruption of the hydrogen bonds existing in the Pcs and DMSO molecules. As a result, TBIT-Pc and TBTT-Pc molecules could connect with neighboring molecules and form face-to-face H-aggregates. In the formation process of H-aggregates, H-bonds and π-π interaction may be the dominant factors. Meanwhile, the aggregation extent increased with an increase of the H-bond numbers formed in the self-assembly system. Compared with TBTT-Pc, there were much more H-bonds in the TBIT-Pc H-aggregates. Therefore, larger size nanoaggregates as shown in the pictures of Fig.3 and TEM images were formed in the DMSO/water mixture of TBIT-Pc than TBTT-Pc.

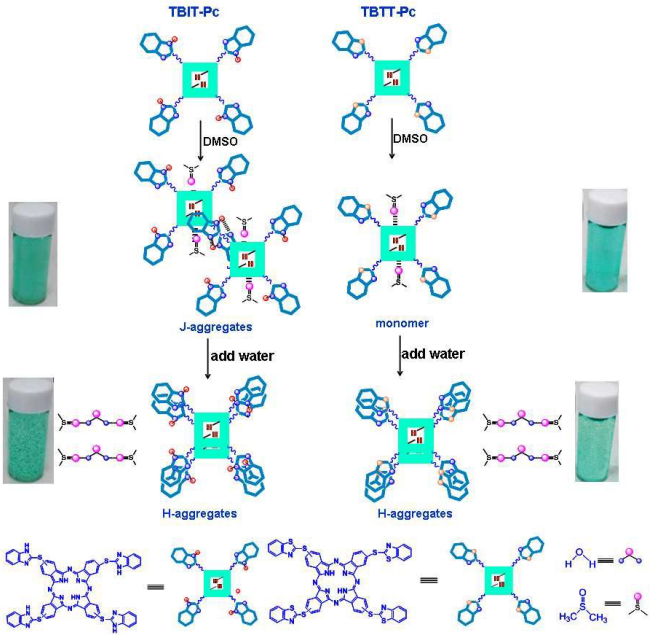

Fig.8. Schematic illustration for the formation process of TBIT-Pc J-aggregates formed in DMSO and H-aggregates formed in DMSO/water mixed solution of TBIT-Pc and TBTT-Pc.

Current-Voltage (I-V) properties

The uniform aggregates of TBIT-Pc and TBTT-Pc with well-defined nanoparticles and dendritic nanostructures may be promising candidates for applications in electronic devices, which depends on the combination of π-π stacking interactions and H-bonds between different Pcs molecules. To demonstrate the semiconducting potentials of these nanostructures, the J and H -type nanoaggregates were carefully pressed onto 60 μm-spaced Au electrodes to study their current-voltage properties. Fig.9 showed the current-voltage (I-V) characteristics of nanoparticles (a), short and long dendritic nanostructures (b and c), respectively. The electronic conductivity extracted from the quasi-linear region at low bias (up to 40 V) was calculated to be around 2.09×10^{-6}, 6.14×10^{-6} and 7.90×10^{-5} S m^{-1} for the nanoparticles, short and long dendritic nanostructures, respectively. In particular, the long dendritic nanostructures of TBIT-Pc showed the highest conductivity in comparison with nanoparticles and short dendritic nanostructures. The short dendritic nanostructures had a better semiconducting ability than nanoparticles. The improved semiconducting property of TBIT-Pc H-aggregates (long dendritic nanostructures) was enhanced by π–π stacking and the additional introduction of hydrogen bonding (N-H···N) between benzimidazole substitutes of TBIT-Pc molecules.[59,60]

Conclusions

Two new metal-free tetra{[1H-benzo(*d*)imidazol-2-yl]thiol}phthalocyanine (TBIT-Pc) and tetra{[benzo(*d*)thiazol-2-yl]thiol}phthalocyanine (TBTT-Pc) have been designed and synthesized in the present paper. TPIT-Pc and TBTT-Pc exhibited excellent solubility in THF, DMF and DMSO. The self-assembly behaviors of TPIT-Pc and TBTT-Pc in solutions were comparatively studied for the first time. TBIT-Pc and TBTT-Pc did not show self-assembly tendency in the solution of DMF. TBTT-Pc was also present as monomer in DMSO. While "head-to-tail" stacking mode self-assemblies (J-aggregates) were formed in the DMSO solution of TBIT-Pc due to the presence of hydrogen bonding (N-H···N) between benzimidazole substitutes. Further comparative investigation of the self-assembly behavior of TBIT-Pc and TBTT-Pc revealed that the H-aggregates were formed in the DMSO/water mixture. In the formation process of aggregates, H-bonds and π-π interaction may be the dominant factors. The degree of H-aggregation increased with more hydrogen bonds (N-H···N) formed. And especially, these results implied the effective effect of hydrogen bonding (N-H···N) introduced in the substituents of TBIT-Pc on the stacking mode, size, morphology and I-V properties of self-assembled nanostructures. The reported benzoxazole-substituted phthalocyanines can be also significant in the applications of optical pH-sensors, optoelectronic devices, photodynamic therapy (PDT) and nanoscale catalysts. Further studies with the novel phthalocyanines and their aggregates will be conducted on these application areas.

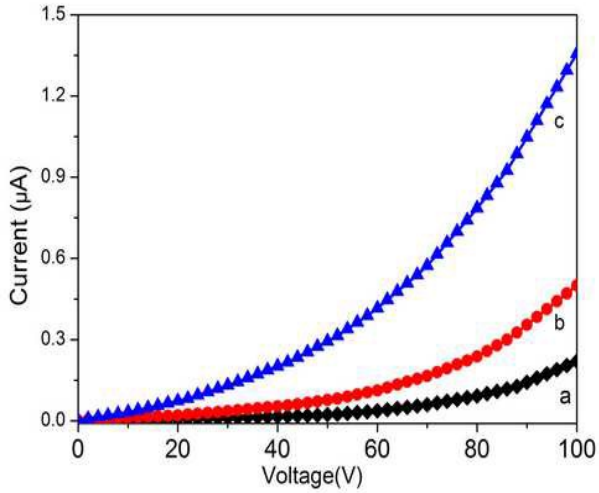

Fig.9. *I–V* curves measured for nanoparticles fabricated from DMSO solutions of TBIT-Pc (a), short and long dendritic nanostructures formed in DMSO/water mixture of TBTT-Pc (b) and TBIT-Pc (c).

Acknowledgements

The authors would like to thank the National Natural Science Foundation of China (No. 21376265) for financial support and the Fundamental Research Funds for the Central Universities (No. 15CX02029A).

Notes and references

State Key Laboratory of Heavy Oil Processing, China University of Petroleum (East China), Qingdao 266580, China. Tel.: +8653286981869;fax: +8653286981787.E-mail address: xiadh@upc.edu.cn (D. Xia).

1 (a) S. Huang, L. Dai, A. W. H. Mau, *J. Phys. Chem. B*, 1999, **103**, 4223–4227; (b) M. Hanack, M. Lang, *Adv. Mater.*, 1994, **6**, 819–833; (c) P. Matlaba, T. Nyokong, *Polyhedron*, 2002, **21**, 2463–2472.

2 T. M. M. Kumar, B. N. Ahcar, *J. Organomet. Chem.*, 2006, **691**, 331–336.
3 J. P. Viricelle, A. Pauly, L. Mazet, J. M. Bouvet, C. Varenne, C. Pijolat, *Mater. Sci. Eng. C.*, 2006, **26**, 186–195.
4 C. C. Leznoff, A. B. P. Lever, In Phthalocyanine: Properties and Applications; VCH: New York, 1993; Vol. 3.
5 F. Moser, H. A. L. Thomas, Phthalocyanine Compounds; Reinhold Publ: New York, 1963.
6 C. C. Leznoff, A. B. P. Lever, Phthalocyanines properties and applications, VCH: New York, 1989; Vol. 1.
7 A. Suchan, J. Nackiewicz, Z. Hnatejko, W. Waclawek, S. Lis, *Dyes and Pigments*, 2009, **80**, 239–244.
8 V. Parra, M. Bouvet, J. Brunet, M. L. Rodríguez-Méndez, J.A. Saja, *Thin Solid Films*, 2008, **516**, 9012–9019.
9 M. Bouvet, *Analytical and Bioanalytical Chemistry*, 2006, **384**, 366–373.
10 G. De La Torre, P. Vazquez, F. Agullo-Lopez, T. Torres, Journal of Materials Chemistry, 1998, **8**, 1671–1683.
11 F. Yang, S.R. Forrest, *ACS Nano*, 2008, **2**, 1022–1032.
12 A. Bilgin, B. Ertem, Y. Gök, *Polyhedron*, 2005, **24**, 1117–1124.
13 M. Emmelius, G. Pawlowski, H.W. Vollmann, *Angewandte Chemie International Edition*, 1989, **28**, 1445–1471.
14 F. Yílmaz, M. Özer, İ. Kani, Ö. Bekaroglu, *Catalysis Letters*, 2009, **130**, 642–647.
15 I. Rosenthal, *Photochemistry and Photobiology*, 1991, **53**, 859–870.
16 R. L. Wershaw, *Soil Sci.* 1999, **164**, 803−813.
17 W. Wang, *Int. J. Pharm*. 2005, **289**, 1−30.
18 Z. Y. Yang, L. H. Gan, S. B. Lei, L. J. Wan, C. Wang, J. Z. Jiang, *J. Phys. Chem. B*, 2005, **109**, 19859−19865.
19 (a) W. J. Schutte, M. Sluyters-Rehbach, J. H. Sluyters, *J. Phys. Chem.*, 1993, **97**, 6069-6073. (b) E. J. Osburn, L. K. Chau, S. Y. Chen, N. Collins, D. F. O'Brien, N. R. Armstrong, *Langmuir*, 1996, **12**, 4784−4796.
20 M. V Martinez-Diaz, M. S. Rodriguez-Morgade, M. C. Feiters, P. J. M. van Kan, R. J. M. Nolte, J. F. Stoddart, T. Torres, *Org. Lett.*, 2000, **2**, 1057−1060.
21 A. Escosura, M. V. Martínez-Díaz, P. Thordarson, A. E. Rowan, R. J. M Nolte, T. Torres, *J. Am. Chem. Soc.*, 2003, **125**, 12300−12308.
22 M. Kasha, H. R. Rawls, M. A. El-Bayoumi, *Pure Appl. Chem.* 1965, **11**, 371−392.
23 S. Kakade, R. Ghosh, .D. K. Palit, *J. Phys. Chem. C*, 2012, **116**, 15155−15166.
24 J. S. Shirk, R. G. S. Pong, S. R. Flom, H. Heckmann, M. Hanack, *J. Phys. Chem. A.*, 2000, **104**, 1438−1449.
25 A. H. Herz, *Adv. Colloid Interface Sci.*, 1977, **8**, 237−298.
26 X.F. Zhang, Q. Xi , J. Zhao. *J. Mater. Chem.*, 2010, **20**, 6726–6733.
27 Q. X. Shi, K.-E. Bergquist, R. P. Huo, J. L. Li, M. Lund,R. Vácha, A. Sundin, E. Butkus, E. Orentas, K.Wärnmark. *J. Am. Chem. Soc.*, 2013, **135**, 15263−15268.
28 C. Farren, S. FitzGerald, A. Beeby and M. R. Bryce. *Chem. Commun.,* 2002, 572–573.
29 M. Shirakawa, S. Kawano, N. Fujita, K. Sada, S. Shinkai. *J. Org. Chem.*, 2003, **68**, 5037-5044.
30 A. R. Karimi, A. Khodadadi, *Tetrahedron Letters*, 2012, **53**, 5223–5226.
31 N. Nagata, S. Kugimiya, Y. Kobuke, *Chem. Commun.*, 2000, **151**, 1389−1390.
32 E. Önal, F. Dumoulin, and C. Hirel, *J. Porphyr. Phthalocya.,* 2009, **13**, 702-711.
33 M. Morisue, K. Ogawa, K. Kamada, K. Ohtab, Y. Kobuke, *Chem. Commun.*, 2010, **46** 2121−2123.
34 M. E. El-Khouly, L. M. Rogers, M. E. Zandler, G. Suresh, M. Fujitsuka, O. Ito, F.D. Souza, *ChemPhysChem*, 2003, **4**, 474−481.
35 K. Kameyama, A. Satake, Y. Kobuke, *Tetrahedron Letters*, 2004, **45**, 7617−7620.
36 M. Kruk and M. Jaroniec, *Chem. Mater.*, 2003, **15**, 2942–2949.
37 S. Z. Topal, E. Önal, A. G. Gürek and C. Hirel. *Dalton Trans.*, 2013, **42**, 11528−11536.
38 A. M. Sevim, C. I., A. Gül, *Dyes and Pigments*, 2011,**89**, 162−168.
39 Y. Gök, H. Kantekin, *Supramol. Chem.*, 2003, **15**, 335−343.
40 B. Akkurt, E. Hamuryudan, *Dyes and Pigments*, 2008, **79**, 153−158.
41 H. Y. Yenilmez, A. İ. Okur, A. Gül, *J. Organomet. Chem.*, 2007, **692**, 940−945.
42 M. Durmus, S. Yes, B. Çosut, A. G. Gürek, A. Kìlìç, V. Ahsen, *Synth. Met*., 2010, **160**, 436−444.
43 A. T. Bilgicli, A. Gunsel, M. Kandaz, A. R. Ozkaya. *Dalton Trans*, 2012, **41**, 7047-7056.
44 X. Huang, F. Q. Zhao, Z. Y. Li, Y. W. Tang, F. S. Zhang, C. H. Tung, *Langmuir*, 2007, **23**, 5167-5172.
45 A. K. Burat, Z. P. Öz, Z. A. Bayır, *Monatsh Chem.*, 2012, **143**, 437–442.
46 C. C. Leznoff, A. B. P. Lever, Phthalocyanines properties and applications, VCH: New York, 1996; Vol. 4.
47 A. T. Bilgicli, M. N. Yarasir, M. Kandaz, A. R. Ozkaya. *Polyhedron*, 2010, **29**, 2498-2510.
48 D. Wohrle, M. Eskes, K. Shigehara, A. Yamada, *Synthesis Stuttgart*, 1993, 194–196.
49 G. Pawlowski, M. Hanack, Synthesis, 1980, **4**, 287–288.
50 A. Lyubimtsev, Z. Iqbala, G. Cruciusa, S. Syrbub, E. S. Taraymovich, T. Ziegler, *J Porphyrins Phthalocyanines*, 2011, **15**, 39–46.
51 X. Y. Li, D. K. P. Ng, *Tetrahedron Letters*, 2001, **42**, 305–309.
52 A. W. Snow, in The Porphyrin Handbook, ed. K. M. Kadish, K. M. Smith and R. Guilard, Academic Press, Amsterdam, 2003, 129–176.
53 Z. Bıyıklıôglu, M. Durmus, H. Kantekin, *Journal of Photochemistry and Photobiology A: Chemistry*, 2011, **222**, 87–96.
54 M. Kimura, T. Muto, H. Takimoto, K. Wada, K. Ohta, K. Hanabusa, H. Shirai and N. Kobayashi, Langmuir, 2000, **16**, 2078–2082.
55 R. Bayrak, H. T. Akçay, M. Durmus, İ. Değirmencioğlu. *Journal of Organometallic Chemistry*, 2011, **696**, 3807–3815.
56 M. Kasha, H. R. Rawls, M. A. EI-Bayoumi, *Pure Appl Chem*, 1965, **11**, 371–392.
57 N. Kobayashi, Y. Higashi, T. Osa, *Chem. Lett.* 1994, 1813–1816.
58 G. Verma, V. K. Aswal, G. Fritz-Popovski, C. P. Shah, M. Kumar, P. A. Hassan, *J. Colloid Interface Sci.*, 2011, **359**, 163−170.
59 Z. Wang, C. J. Medforth, C. J. Shelnutt, *J. Am. Chem. Soc.*, 2004, **126**, 15954–15955.
60 Y. Chen, Y. Feng, J. Gao, M. Bouvet, *J. Colloid Interface Sci.*, 2012, **368**, 387–394.

GA

Novel metal-free tetra{1H-benzo[d]imidazol-2-yl)thiol}phthalocyanine (TBIT-Pc) and tetra{(benzo[d]thiazol-2-yl)thiol}phthalocyaninate (TBTT-Pc) were synthesized and characterized. TBIT-Pc self-assembled to J-aggregates and H-aggregates in DMSO and DMSO/water, while TBTT-Pc was present as monomer and H-aggregates in DMSO and DMSO/water.